

Site-Specific BER Analysis in Frequency-Selective Channels Using a Ray-Tracing Propagation Model

Harry R. Anderson¹
EDX Engineering, Inc.
P.O. Box 1547
Eugene, Oregon 97440
Tel: (503) 345-0019 FAX: (503) 345-8145

Abstract - A technique is presented for calculating the bit error rate (BER) for coherent QPSK in frequency-selective channels using site-specific channel response characteristics. The details of the channel response are found from a ray-tracing propagation model which provides unique, realistic fading-dependent time signatures for each analysis location in the propagation environment. The channel time signatures are used for a direct estimate of intersymbol interference (ISI) which can then yield an estimate of wideband BER. The technique offers a more incisive calculation of BER in frequency-selective channels for real propagation circumstances than is possible with previously-used methods. The technique can be adapted to other modulation types and general co-channel interference problems.

1. Introduction

The increasing use of wideband digital communication systems has placed new requirements on the channel models which are used to assess system performance. "Wideband" in this case is generally thought of as any system in which the occupied transmission bandwidth is much greater than the coherence bandwidth of the channel. The coherence bandwidth of the channel is a function of the time dispersion of energy in the channel. Coherence bandwidth is often found as the Fourier transform of the power delay profile which shows the degree of delay and time spreading a digital pulse experiences in transit from the transmitter to the receiver. The time dispersion is directly a function of the characteristics of the propagation environment. A line-of-sight system in free space experiences no time dispersion, while systems operating in complex urban propagation environments will experience substantial time dispersion. Depending on system type, design, and data rate, time dispersion rather than signal-to-noise ratio (SNR) may ultimately determine the limits of system performance.

Time dispersion of transmitted symbols leads to intersymbol interference since the delayed energy from a preceding symbol pulse will be seen as interference at the sample time for subsequent pulses. Attempts at finding the resulting ISI have variously been based on some assumed channel energy distribution. So-called two-ray and multi-ray models have been used to represent the channel energy where relative ray amplitudes and phases are either randomly assigned, assigned based on simple two-ray or multi-ray model assumptions, or assigned to follow some simple exponential function which decays with time. The weakness of this approach is that the channel energy distribution is hypothetical and not necessarily a good representation of the wide variety of channel response conditions which will be encountered in real propagation environments. Also, when the power distribution (power delay profile) only is considered using the RMS delay spread, no phase information is available so no assessment of the extent of frequency-selective fading on BER can be made. This is the main weakness of attempting to do frequency-selective BER analysis using a single number like RMS delay spread - it does not convey many important details about the time and local spatial dependence of the channel response.

Recent work has improved the approach to wideband BER analysis by relating the fading characteristics of a pilot tone on the channel carrier frequency to BER for a given RMS delay spread. [1]. While this finally does provide a fading-dependent BER result, it still does not account for frequency-selective fades off the carrier frequency. Also, the particular implementation reported in [1] is based on Monte Carlo simulation. Only a few representative channel response models were used to develop the relationship between RMS delay spread and fade depth. To find truly site-specific BER estimates, the simulation would have to be run for each site's channel response, a process which is not computationally convenient when performance estimates throughout a microcell service area are required.

Using a ray-tracing propagation model, very specific information can be found about the amplitude, phase, and time delay characteristics of any set of points in the

¹ This research was done while the author was resident at the Centre for Communications Research at the University of Bristol.

propagation environment for the intended system service area. In the technique presented here, this specific information is used to directly assess the fading statistics of both the desired symbol pulse and the delayed interfering symbol pulses at the detector sampling instant. From these statistics, and introducing additive white gaussian noise (AWGN) on the signal, a direct calculation of both burst and average wideband BER is possible.

2. Channel Response Model Using Ray-Tracing

A general model for the low-pass impulse response for an urban radio channel is:

$$h(t) = \sum_{n=1}^N A_n \delta(t - \tau_n) \exp(-j(\theta_n + \Delta\theta_n)) \quad (1)$$

in which the impulse response $h(t)$ is the sum of a set of N impulses arriving at delay times τ_n with amplitudes A_n , phases θ_n , and phase displacement $\Delta\theta_n$. The phase displacements result from the motion of the receiver or other spatial change of the receiver location relative to the rest of the propagation environment which may itself include moving objects (reflections from cars and buses, etc.). For a mobile receiver the displacement term is given by $\Delta\theta_n = (2\pi vt / \lambda) \cos(\phi_n + \phi_v)$, where ϕ_n is the arrival angle of the n^{th} impulse, v is the speed of motion, and ϕ_v is the direction of motion.

To use this model, it is necessary to identify the amplitudes, time delays, and absolute phase shifts of the N components of $h(t)$. The received components may consist of the line-of-sight signal from the transmitter and a variety of signals reaching the receive antenna via reflection surfaces, diffracting corners and scattering surfaces. By using ray-tracing techniques, the energy emitted from the source transmitting antenna is geometrically traced to determine those surfaces or corners which are illuminated. For the ray-tracing model used here, each illuminated surface is replaced by an image transmitter or scattering source such that the radiation from the image represents (in amplitude, phase, and radiating directions) the energy reflected from the source. Similarly, an illuminated corner is replaced by an equivalent wedge diffraction source. With the first set of images and illuminated corners in place, each of them is then considered in turn by ray-tracing to determine the surfaces and corners they illuminate. This process is repeated for as many iterations as may be relevant to the problem at hand, or which are practical from a computational point of view. The ray interactions with the propagation environment are tracked for both HP and VP by taking into account the conductivity and permittivity of the walls and corners, and the angle of incidence for the interaction at each wall and corner. A typical ray tracing study for a transmitter at point AA to a receiver at point R is

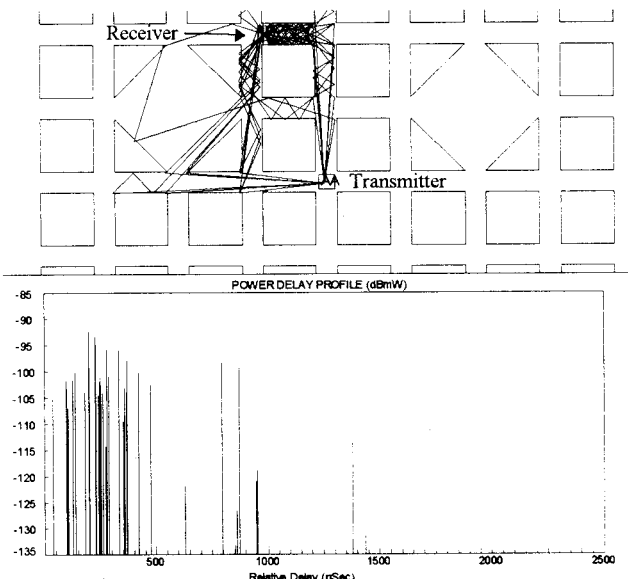


Fig. 1. Ray-tracing study with power delay profile.

shown in Figure 1 along with the resulting power delay profile. As shown in [2], the magnitude and phase of the reflection coefficient will be a strong function of the angle of incidence on the reflecting surface.

A ray-tracing propagation model only provides the ray amplitudes and phases to a single precise point. At this point it may happen that the vector sum of the rays result in a null (fade) or peak in the voltage envelope. However, in general the geometry of the environment is not known with sufficient accuracy to predict the phase of the envelope voltage precisely. The carrier frequencies typically involved in PCS microcell systems (around 2000 MHz) the wavelength is on the order 15 cm. In a typical urban building database, the building wall locations may only be known within perhaps one meter. Because absolute phase can't be known, it is necessary to determine the channel response over a range of positions around the precise location where the ray-tracing analysis was performed. This can be done by considering a number of *time signatures* representing the channel response over a range of wavelength displacements around this point. In this analysis, the time signatures are determined by taking points every 0.0625 wavelengths along the circumference of a circle of sample points. The circumference of the sampling circle is typically set at 10λ or 20λ , resulting in from 160 to 320 channel response sample points for each ray-tracing study points. This uniform circular pattern of sample points is used to reduce any anomalies which might result from the location of the point relative to the physical environment and the particular arrival angles of the rays.

3. Time Signature of Received Voltage

When a data symbol waveform $u(t)$ is transmitted, the resulting received voltage is:

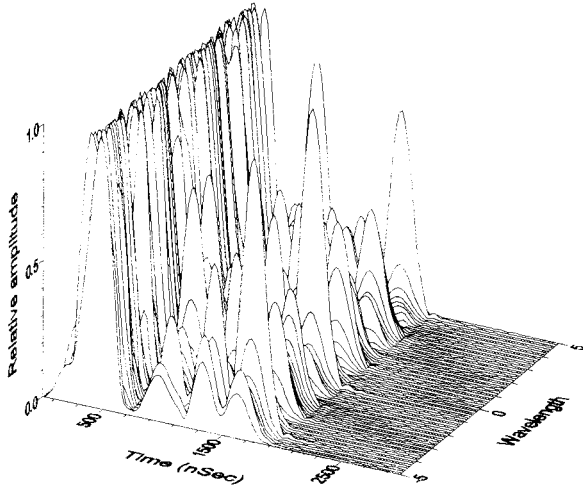


Fig. 2. Time signatures for ray-tracing analysis point.

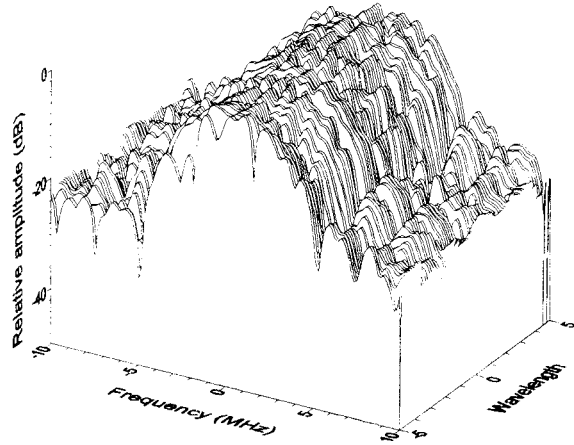


Fig. 3. Spectrum signatures for ray-tracing analysis point shown in Figure 2.

$$r(t) = \sum_{n=1}^N A_n u(t - \tau_n) \exp(-j(\theta_n + \Delta\theta_n)) + n(t) \quad (2)$$

where $n(t)$ is the AWGN. For the studies done here, $u(t)$ was assumed to be the usual raised-cosine pulse:

$$u(t) = \frac{\sin(\pi/T)}{\pi/T} \frac{\cos(\beta\pi/T)}{(1-4\beta^2 t^2/T^2)} \quad (3)$$

This is essentially a sinc function pulse. The pulse shape parameter β is set to 1.0 for the studies done here.

With a particular modulation type and data rate, the time signature of the channel for a given value of phase displacement or spatial displacement along a sampling circle can be found from (2). A sequence of such time signatures can be assembled by re-computing $r(t)$ at each point on the sampling circle. An example of such a sequence of time

signatures around the sampling circle with a 10 λ circumference is shown in Figure 2 where the modulation is a 5 Mbps QPSK signal using the raised cosine pulse shape. The inter-symbol interference (ISI) due to pulse spreading, and the dynamic nature of the channel response when moving around the sampling circle, is clear. It's this type of detail which a single number like RMS delay spread cannot take into account. The RMS delay spread of the power delay profile is exactly the same for each of the time signatures in Figure 2, yet the intersymbol interference in each case will be different. The corresponding spectrum signatures for the same set sampling circle are shown in Figure 3. The data in Figure 3 was developed by taking the FFT of the time signatures in Figure 2.

From the time signature sequence like that in Figure 2, a distribution of the ISI voltage can be found by assembling the signature sample values at the interfering timing point and constructing an estimated probability distribution from them. In constructing the distribution of the ISI voltage, it should be recognized that interference will occur not only from the pulse immediately prior to the pulse being detected, but theoretically also from all the other transmitted pulses. The nature and extent of the time dispersion in the channel will determine how many other pulses are relevant. In some propagation circumstances, isolated, long-delayed echoes from distant buildings may represent the controlling factor on BER and any wideband BER analysis method should be capable of accommodating such long-delayed interference. Also, depending on the modulation signal constellation, the code sequence for the other pulses will also be important to the distribution of the ISI. At sampling time t_k the summation of the ISI voltages $b(t_k)$ from all other pulses can be written as:

$$b(t_k) = \sum_{m=-\infty}^{\infty} r(t_k - mT_s) \quad m \neq 0 \quad (4)$$

For $m=0$, $r(t)$ is the desired pulse and not part of the interference. The values of $r(t)$ are treated as complex voltages so $b(t_k)$ is the vector sum of the echo pulses.

Equation (4) gives a site-specific calculation of the ISI voltage which explicitly takes into account the multipath conditions present at a given study point. It will allow a direct calculation of the wideband, frequency selective burst and average BER as explained in the section 5.

The calculation of the ISI in (4) is highly dependent on the sample times t_k . Establishing a sample timing point can be done in many ways. For the research done here, the sample time was established by selecting the maximum point on a given time signature as the desired symbol sampling instant, and finding the timing points for the interfering voltages at $\pm mT_s$ from this reference time. Since it is assumed that a given time signature represents the channel response for several symbol periods, this is essentially a quasi-static approach to error analysis.

4. BER of Coherent QPSK With Interference

Finding the symbol error for coherent M -PSK with AWGN and constant amplitude sinuswave interference is a classic problem which was addressed many years ago (see, for example [3], [4], and [5]). The similar approach was used in [6] for atmospheric noise. Using straightforward vector geometry for the desired signal, noise, and interference, and assuming the phase of the interference is random and uniformly distributed but with constant amplitude, the technique constructs an equation for the probability density of the phase α given the noise and interference level. The general equation for the phase distribution with noise and interference as taken from [6] is:

$$p(\alpha) = \frac{1}{2\pi\sigma^2} \int_0^\infty \exp\left[-\frac{1}{2\sigma^2}(r^2 + b^2 + 1 - 2r \cos \alpha)\right] \times I_0\left[\frac{b}{\sigma^2}(r^2 + 1 - 2r \cos \alpha)^{1/2}\right] r dr \quad (5)$$

$$\text{where: } \sigma = \frac{1}{\sqrt{2}} 10^{-(\text{SNR})/20} \quad \text{and} \quad b = 10^{-(\text{SIR}/20)}$$

with SNR the signal-to-noise ratio in dB and SIR the signal-to-interference ratio in dB. The integral in (3) can be solved numerically for a selection of SNR and SIR values resulting in detected phase pdf's like those shown in Figure 4 (assuming a noise-free phase reference for detection). A symbol error occurs in coherent QPSK when the detected phase falls outside the region $\pm \pi/4$, corresponding to the area under the curve in Figure 4 outside $\pm \pi/4$. Using this approach, the BER for coherent QPSK for several values of

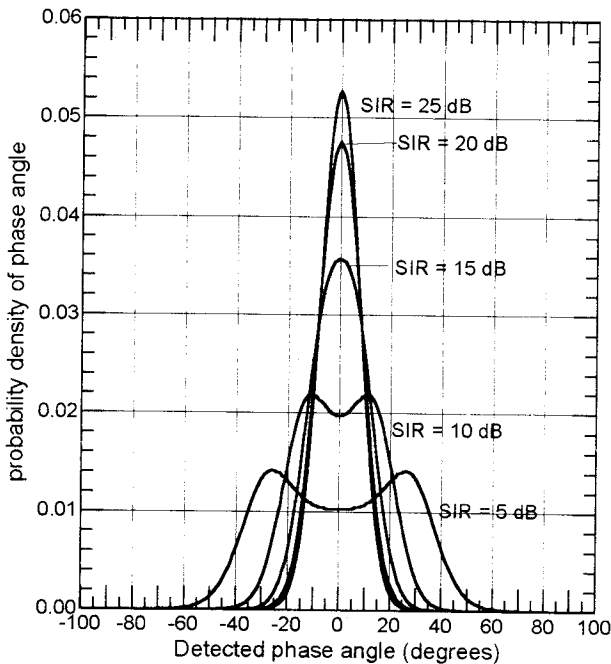


Fig. 4. Probability density (pdf) of phase (SNR=15 dB)

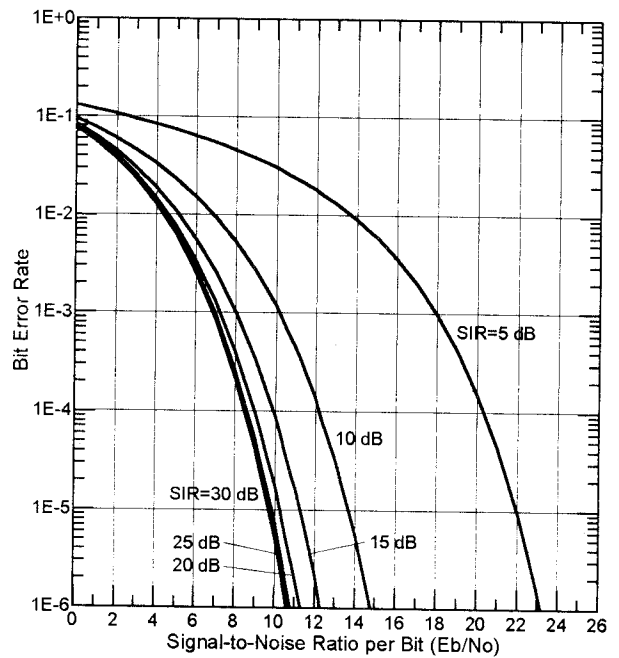


Fig. 5. Bit error probability for coherent QPSK with AWGN and sinuswave interference.

SIR and SNR were calculated and plotted in Figure 5, assuming the QPSK is Gray-coded such that the BER equals half the symbol error rate (SER) [7].

5. Burst and Average Bit Error Rates

The ISI voltage in (4) when considered with the desired symbol amplitude forms the SIR, which, when combined with the BER results from Section 4, yields a BER for a given ISI and noise level. Note that only the ISI amplitude is considered which is consistent with Section 4.

Given that the ISI is explicitly known for a given time signature from the sampling circle, a "burst" error rate for each time signature can be directly calculated. The result of this is shown in Figure 6 versus the narrowband carrier envelope power, SIR and SNR. For the study shown in the Figure 6 the RMS delay spread is 327 nSec and the QPSK data rate is 1 Mbps. As can be seen, the burst error rate is strongly (but not perfectly) correlated with narrowband carrier fade depth which reinforces the premise of the work in [1]. It also shows that the method described here is in close agreement with the Monte Carlo simulation approach used to construct the results in [1]. However, it should be noted that broadband "flat" fades can still sometimes occur when ISI-caused errors don't occur. Conversely, errors can occur even with no narrowband carrier fade due to fading elsewhere in the signal transmission bandwidth.

The average BER at a study point can be constructed as the average of the burst BER's calculated as described above. Alternately, the ISI voltages for the ensemble of time signatures can be viewed as samples from a continuous distribution of ISI values. The samples can be used to

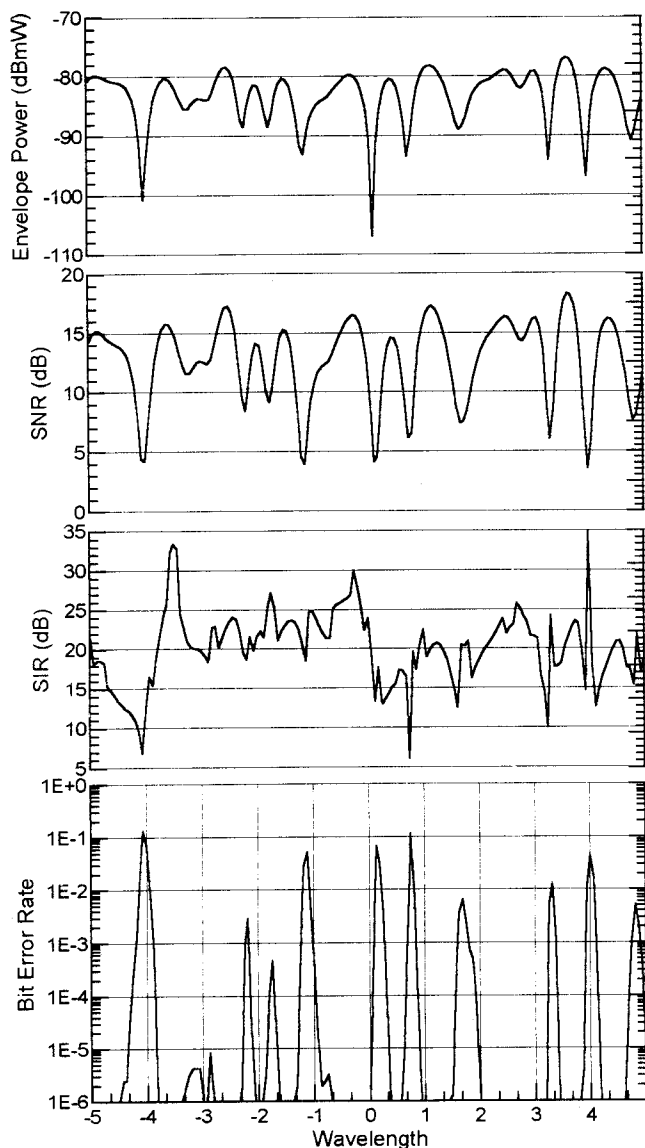


Fig. 6. Burst error rate as a function of fading envelope power, SNR, and SIR.

construct a CDF directly, or the mean and variance of the samples used to postulate a continuous probability distribution. Assuming the pdf of the signal-to-interference ratio is $p(\text{SIR})$, the average error rate at the study point can be written:

$$P_e = \sum_{\text{SIR}} p(\text{SIR}) p(e | \text{SIR}, \text{SNR}) \quad (6)$$

where the summation occurs over a range of practical SIR values, typically 0 dB to 30 dB. The pdf for the error $p(e | \text{SIR}, \text{SNR})$ is found as described in Section 4, and for a practical implementation of this method, could consist of a lookup table of values such as those plotted in Figure 5.

The method presented here can be adapted to other modulation schemes such as differential QPSK by using a different function $p(e | \text{SIR}, \text{SNR})$ in equation (6). With

differential modulation, or coherent modulation where the constellation states have different amplitudes such as 16QAM, the analysis described here could provide an upper bound by assuming the desired symbol was a lowest amplitude signal state and all the other interfering symbols are the highest amplitude states.

6. Conclusions

A method for finding BER in wideband, frequency-selective channels has been presented. The method uses a ray-tracing propagation model to construct realistic channel response signatures which provide a direct computation of ISI voltages as well as estimates of the statistics of the ISI voltage as a function of local fading conditions.

This method for determining wideband BER can be adapted to other modulation schemes by using other pdf's which describe the probability of a bit error as a function of noise and sinewave interference.

Since the ray-tracing propagation model is equally capable of determining the amplitude of interfering pulses arriving from other transmitters, the technique described here could also be generalized to accommodate interference from other sources, such as co-channel mobile units in a CDMA system.

7. Acknowledgment

The author would like to thank Andy Nix of the Centre for Communication Research at the University of Bristol for discussions which were helpful in carrying out this research.

8. References

- [1] A.R. Nix, H.R. Anderson, and J.P. McGeehan, "Estimating Wideband Bit Error Rates Using Pilot Tone Envelope Fading Statistics," *Proceedings of the Fourth International Symposium on Personal, Indoor and Mobile Radio Communications*, Sept. 1993, Yokohama, Japan.
- [2] H.R. Anderson, "A ray-tracing propagation model for digital broadcast systems in urban areas," *IEEE Trans. on Broadcasting*, Vol. 39, no. 3, Sept. 1993, pp. 309-317.
- [3] A.S. Rosenbaum, "PSK Error Performance With Gaussian Noise and Interference," *Bell System Technical Journal*, Vol. 48, pp. 413-442, February, 1969.
- [4] F.E. Glave, "An upper bound on the probability of error due to intersymbol interference for correlated digital signals," *IEEE Trans. on Inform. Theory*, Vol. IT-17, pp. 356-363.
- [5] S. Benedetto, E. Biglieri, and V. Castellani, "Combined effects of intersymbol, interchannel, and co-channel interferences in M-ary CPSK systems," *IEEE Trans. on Commun.*, Vol. COM-21, No. 9, Sept., 1973.
- [6] H.R. Anderson, "Theoretical performance of binary coherent PSK on AM SCA channels," *IEEE Trans. on Broadcasting*, Vol. BC-20, No. 4, Dec. 1983, pp. 113-120.
- [7] J. Proakis. *Digital Communications*. New York: McGraw-Hill, 1989, p. 265.